"Electron pockets in the Fermi surface of hole-doped high-T_c superconductors"

David LeBoeuf [1], Nicolas Doiron-Leyraud [1], R. Daou [1], J.-B. Bonnemaison [1], Julien Levallois [2], N.E. Hussey [3], Cyril Proust [2], L. Balicas [4], B. Ramshaw [5], Ruixing Liang [5,6], D.A. Bonn [5,6], W.N. Hardy [5,6], S. Adachi [7] & Louis Taillefer [1,6]

[1] *Département de physique and RQMP, Université de Sherbrooke, Sherbrooke J1K 2R1, Canada*

[2] *Laboratoire National des Champs Magnétiques Pulsés (LNCMP), UMR CNRS-UPS-INSA 5147, Toulouse 31400, France*

[3] *H.H. Wills Physics Laboratory, University of Bristol, Bristol BS8 1TL, UK*

[4] *National High Magnetic Field Laboratory, Florida State University, Tallahassee, Florida 32306, USA*

[5] *Department of Physics and Astronomy, University of British Columbia, Vancouver V6T 1Z4, Canada*

[6] *Canadian Institute for Advanced Research, Toronto M5G 1Z8, Canada*

[7] *Superconductivity Research Laboratory, International Superconductivity Technology Center, Shinonome 1-10-13, Koto-ku, Tokyo 135-0062, Japan*

Magnetic field – Temperature phase diagrams

In this section, we determine the field scale above which the effects of vortex motion and superconducting fluctuations (of phase or amplitude) have become negligible in R_{xx} and R_{xy}, such that these transport coefficients reflect predominantly the properties of the normal state. This field scale, which we label $B_n(T)$ and define below, is plotted in a B-T diagram for each of the three materials in Figs. S2a to S2c. It is compared to two other curves. The first is $B_S(T)$, the field below which the vortex solid phase exists, *i.e.* the so-called irreversibility field below which $R_{xy}(B, T) = R_{xx}(B, T) = 0$. It is straightforward to obtain B_S from the isotherms of $R_H(B)$ in Fig. 2. In Fig. S3a, the isotherms at $T = 4.2$ K are shown to respectively yield $B_S = 25$, 20 and 37 T, for II, VIII and Y124, with ± 2 T uncertainty. The second curve to which we compare B_n is $T_0(B)$, defined as the temperature at which $R_H(T)$ changes sign, *i.e.* where $R_H(T_0) = 0$, readily obtained from the curves of R_H vs T in Fig. S1. *The key observation is that T_0 is independent of field at the highest fields in all three materials*. This shows that the temperature-induced sign change in R_H at high fields, featured in Fig. 3, is not caused by flux flow (see below). The case is particularly clear in VIII, where the sign change occurs *above* $T_c(0)$ and is totally independent of field over the entire field range from 0 to 45 T (see Fig. S2b). The negative R_H is thus clearly a property of the normal state, the consequence of a drop in $R_H(T)$ which starts below a field-independent temperature T_{max}. The value of T_{max} at the three doping levels studied here is 50, 105 and 60 K, for II, VIII and Y124, respectively, with ± 5 K uncertainty.

Vortex contribution to Hall resistance

It is important to distinguish the field-independent, *temperature-induced* sign change mentioned above, which persists to the highest fields, from the temperature-dependent, *field-induced* sign change that can result from a vortex contribution to σ_{xy}.

The latter has been studied extensively in a number of cuprates[1,2] and it arises from a cancellation of normal-state (σ^{n}_{xy}) and flux-flow (σ^{f}_{xy}) contributions in the total Hall conductivity ($\sigma_{xy} = \sigma^{n}_{xy} + \sigma^{f}_{xy}$) that can occur if the two contributions happen to be of opposite sign. Given the very different field dependencies of the two contributions, a cancellation and sign change in σ_{xy} (and hence in R_{xy}) can only occur at a particular value of B, for any given T. The most compelling argument against this being the mechanism for the high-field sign change in YBCO is provided by the 70-K isotherm in VIII (see Fig. 2b), which is totally flat and nearly zero at all B, *i.e.* $R_H(70\text{ K}) \approx 0$ independent of B. It is indeed unphysical to suppose that a finite σ^{f}_{xy} conspires to remain equal to $-\sigma^{n}_{xy}$ at all B.

A vortex contribution is also observed in our samples, and it makes a *positive* contribution to R_{xy} in all three materials. It is clearly seen in the 4.2 K isotherm of Y124, for example, where it shows up as a small positive overshoot just above $B_S = 37$ T (see Fig. 2c). This vortex-related contribution persists to high temperature, causing a detectable "bump" at low fields up to 50 K or so. In Y124, the low-field regime (in this case below 40 T or so) is dominated by the vortex contribution so that one needs to go above 50 T to uncover the clean normal-state behaviour. The same field-induced positive overshoot is seen in II (Fig. 2a), although not below 20 K, presumably because of the stronger pinning in this non-stoichiometric material. It is instructive to also look at R_H vs T, as in Fig. S1a, for we can see then that the 15 T curve lies *above* the 55 T curve at all T up to 80 K (see Fig. S4a). This excess in $R_H(T)$ relative to the normal state curve, *i.e.*, the difference between the two curves, $R_H(T, 15\text{ T}) - R_H(T, 55\text{ T})$, is the positive vortex contribution, plotted in the inset of Fig. S4a. It persists at temperatures slightly above $T_c(0)$, as one might expect from superconducting fluctuations. In Fig. S4b, this excess is shown to track the reported rise in the Nernst signal, believed to be a measure of vortex fluctuations[3], in a Y123 sample with the same T_c of 57 K (ref. 4). As in all previous studies (see refs. 1 and 2, and references therein), the vortex contribution to R_{xy} is seen to vanish at high fields (see Fig. S1), specifically above 35, 25 and 50 T in II, VIII and Y124, respectively. Note, however, that the effect of vortices appears to remain detectable up to higher fields in the Nernst signal[3] than it does in the Hall signal.

Flux flow does not cause a sign change in VIII. Looking at the *B*-*T* diagrams of Fig. S2, one can see that this is because the $T_0(B)$ line lies completely above the superconducting state in the case of VIII, whereas it intersects the $B_n(T)$ line in the other two materials. The bending of $T_0(B)$ that results from this intersection is what gives the field-induced sign change. In general, flux flow appears to have little impact on R_H in this material.

Magnetic field scales

As in previous high-field studies of cuprates (refs 5, 6), the fields B_s and B_n are respectively defined at low temperature as the field above which $R_{xy}(B)$ departs from zero and the field below which $R_{xy}(B)$ departs from its high-field, roughly linear behaviour. This is illustrated (by arrows) in Fig. S3a for $T = 4.2$ K. Note that this criterion does not work at high temperatures, so instead we use $R_{xx}(B)$ to determine B_s and B_n. At low temperatures, the values obtained by both the longitudinal and transverse resistive components correlate well, as shown in Fig. S3b, giving us confidence in their determination.

[1] Hagen, S.J. *et al.* Anomalous flux-flow Hall effect: $Nd_{1.85}Ce_{0.15}CuO_{4-y}$ and evidence for vortex dynamics. *Phys. Rev. B* **47**, 1064-1068 (1993).

[2] Nagaoka, T. *et al*. Hall anomaly in the superconducting state of high-T_c cuprates: universality in doping dependence. *Phys. Rev. Lett.* **80**, 3594-3597 (1998).

[3] Wang, Y. *et al*. High field phase diagram of cuprates derived from the Nernst effect. *Phys. Rev. Lett.* **88**, 257003 (2002).

[4] Rullier-Albenque, F. *et al*. Nernst effect and disorder in the normal state of high-T_c cuprates. *Phys. Rev. Lett.* **96**, 067002 (2006).

[5] Balakirev, F.F. *et al.* Signature of optimal doping in Hall-effect measurements on a high-temperature superconductor. *Nature* **424**, 912-915 (2003).

[6] Balakirev, F.F. *et al.* Magneto-transport in LSCO high-T_c superconducting thin films. *New J. of Phys.* **8**, 194 (2006).

[7] Huntley, D.J. & Frindt, R.F. Transport properties of $NbSe_2$. *Can. J. Phys.* **52**, 861-867 (1974).

Figure S1 | Hall coefficient vs temperature.

Hall coefficient $R_H = t\,R_{xy} / B$ as a function of temperature T at different fields as indicated for **a)** Y123 ortho-II (y = 6.51; p = 0.10); **b)** Y123 ortho-VIII (y = 6.67; p = 0.12); **c)** Y124 (p = 0.14).

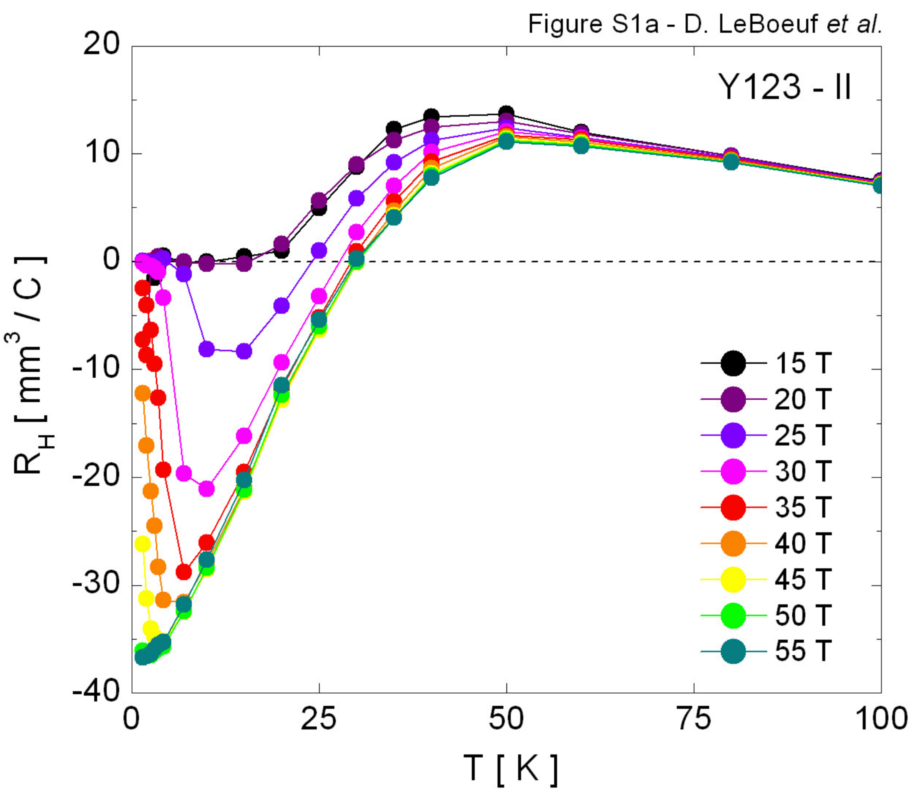

Figure S1b - D. LeBoeuf *et al.*

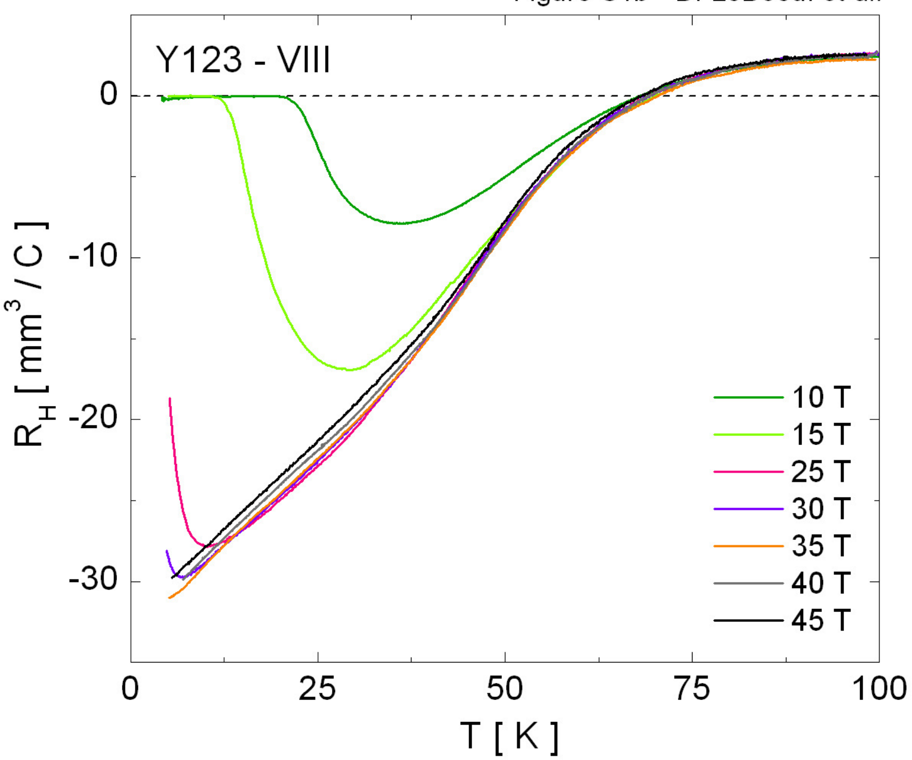

Figure S1c - D. LeBoeuf *et al.*

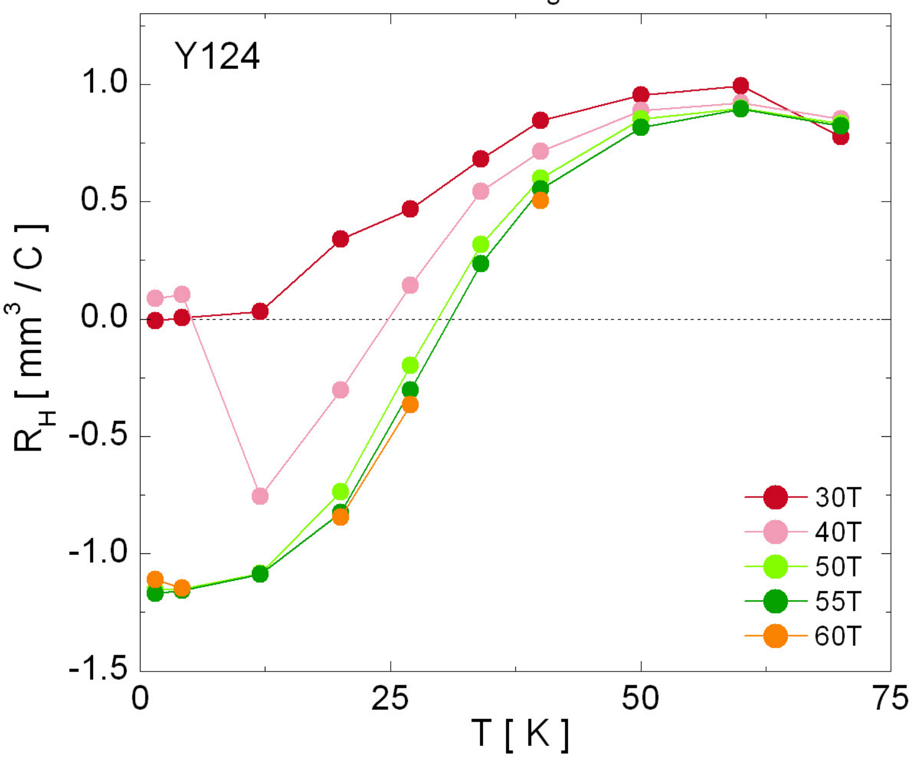

Figure S2 | Magnetic field - Temperature phase diagram.

B – *T* phase diagram for: **a)** Y123 ortho-II (p = 0.10); **b)** Y123 ortho-VIII (p = 0.12); **c)** Y124 (p = 0.14). The vortex solid phase ends at $B_s(T)$ and the transport properties of the normal state are reached above $B_n(T)$, where vortex contributions to transport are negligible. $B_s(T)$ and $B_n(T)$ are defined via R_{xx} (circles) or R_H (squares) vs B, as described in the text and shown in Figs. S3a and S3b. Red circles mark $T_0(B)$, the temperature where R_H changes sign.

Figure S2a - D. LeBoeuf *et al.*

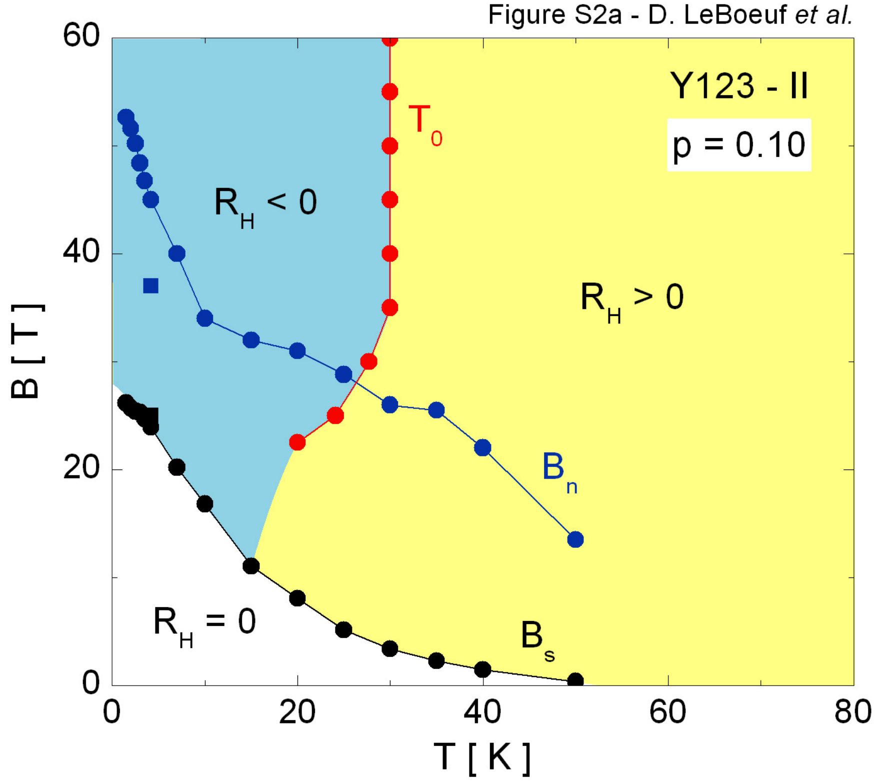

Figure S2b - D. LeBoeuf *et al.*

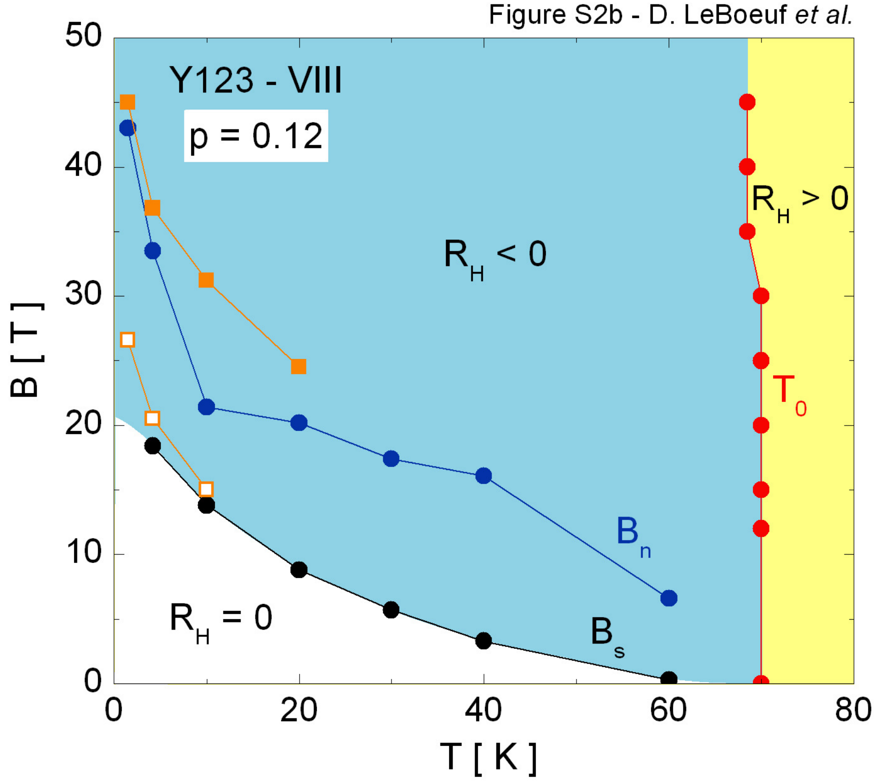

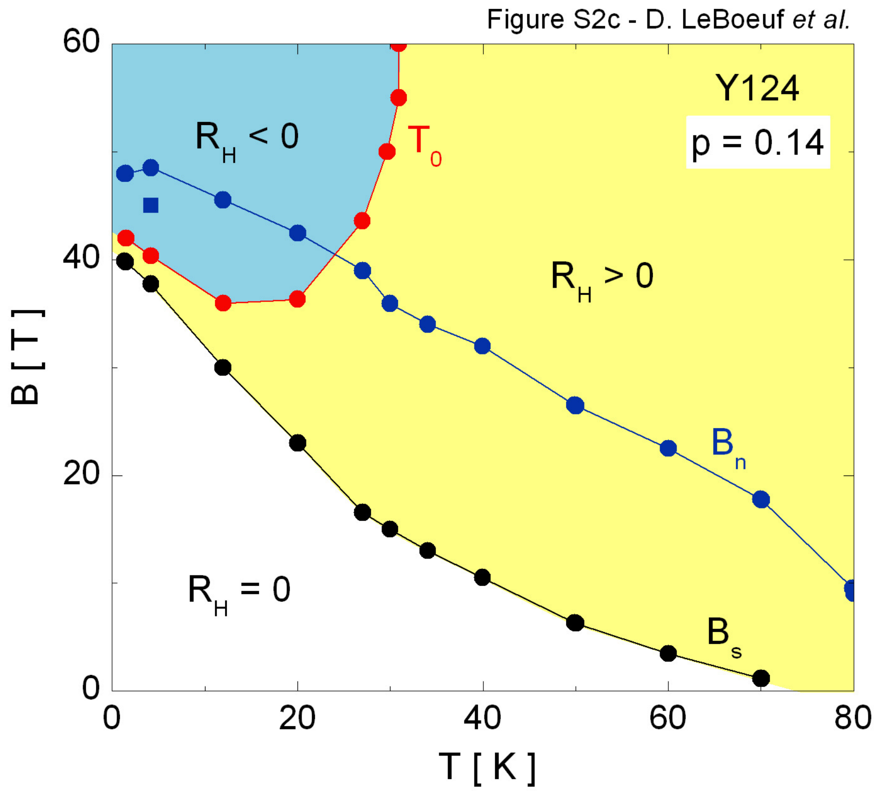
Figure S2c - D. LeBoeuf et al.
Y124
p = 0.14
R_H < 0
T_0
R_H > 0
B_n
R_H = 0
B_s
B [T]
T [K]
0
20
40
60
80

Figure S3 | Determination of magnetic field scales.

a) Hall coefficient $R_H = t\, R_{xy} / B$ as a function of magnetic field B at 4.2 K for Y123 ortho-II (p = 0.10), Y123 ortho-VIII (p = 0.12), and Y124 (p = 0.14). The arrows mark the field B_s above which R_H departs from zero and the field B_n below which R_H deviates from the high-field behaviour of a nearly flat R_H (the fact that the normal-state R_H in II and VIII shows some field dependence is consistent with the two-carrier picture discussed in the text). The values of B_s and B_n thus obtained are shown as squares in Figs. S2a to S2c. (Note that the data shown here for II comes from a different sample to that shown in Fig. 2a, one in which the transition at B_n is sharper and thus more easily defined.) **b)** Longitudinal resistance R_{xx} as a function of field at different temperatures for Y123 ortho-VIII (offset for clarity). The arrows indicate the values for B_n obtained from R_H in a) and in Fig. 2b, showing a good correlation with the field below which R_{xx} departs from its high-field behaviour of a roughly linear magneto-resistance (fitted to a dashed line). The values of B_n thus obtained from R_{xx} are shown as circles in Figs. S2a to S2c.

Figure S3a - D. LeBoeuf *et al.*

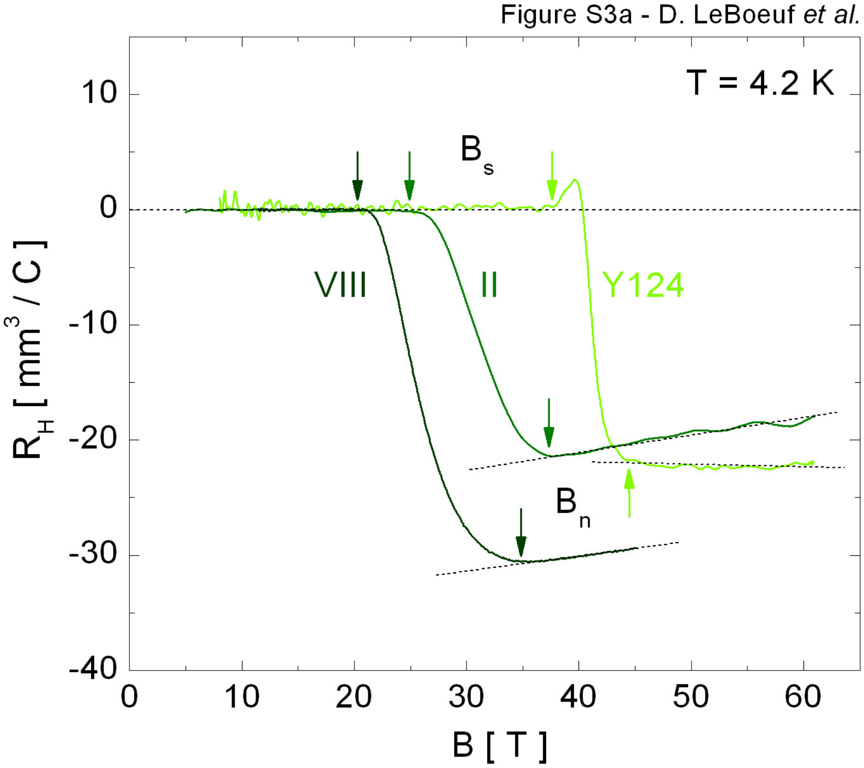

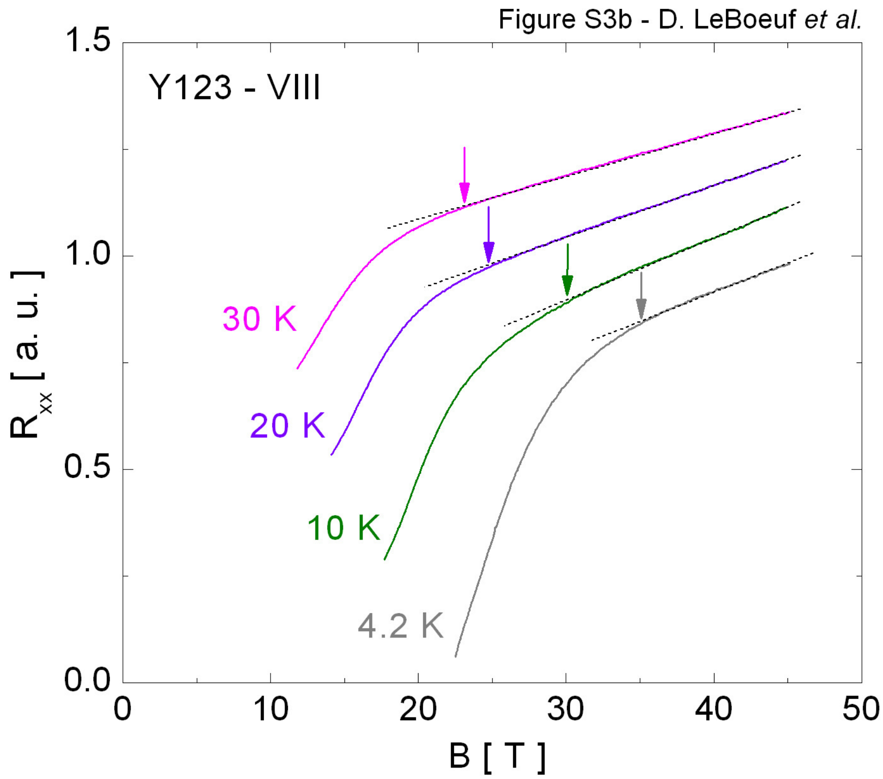
Figure S3b - D. LeBoeuf *et al.*
Y123 - VIII
30 K
20 K
10 K
4.2 K
1.5
1.0
0.5
0.0
R_{xx} [a. u.]
0
10
20
30
40
50
B [T]

Figure S4 | Vortex contribution to Hall coefficient.

a) Hall coefficient $R_H = t\,R_{xy} / B$ as a function of temperature T at 15 and 55 T for Y123 ortho-II. Inset: Difference $\Delta R_H = R_H(15T) - R_H(55T)$ between the two curves shown in the main panel. **b)** Difference $\Delta R_H = R_H(15T) - R_H(55T)$ (left scale) and Nernst signal at 8 T on Y123 with $p = 0.10$ (right scale, from ref. 4) as a function of temperature, showing that the positive difference between $R_H(15T)$ and $R_H(55T)$ is caused by a vortex (flux-flow) contribution to the Hall coefficient at low field.

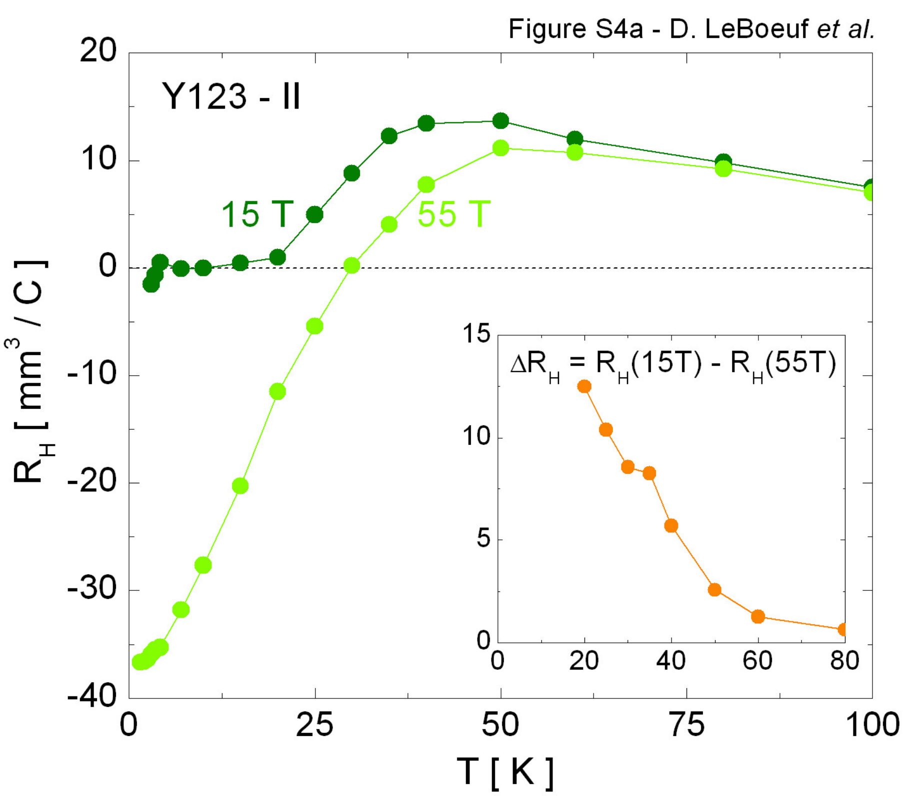

Figure S4b - D. LeBoeuf *et al.*

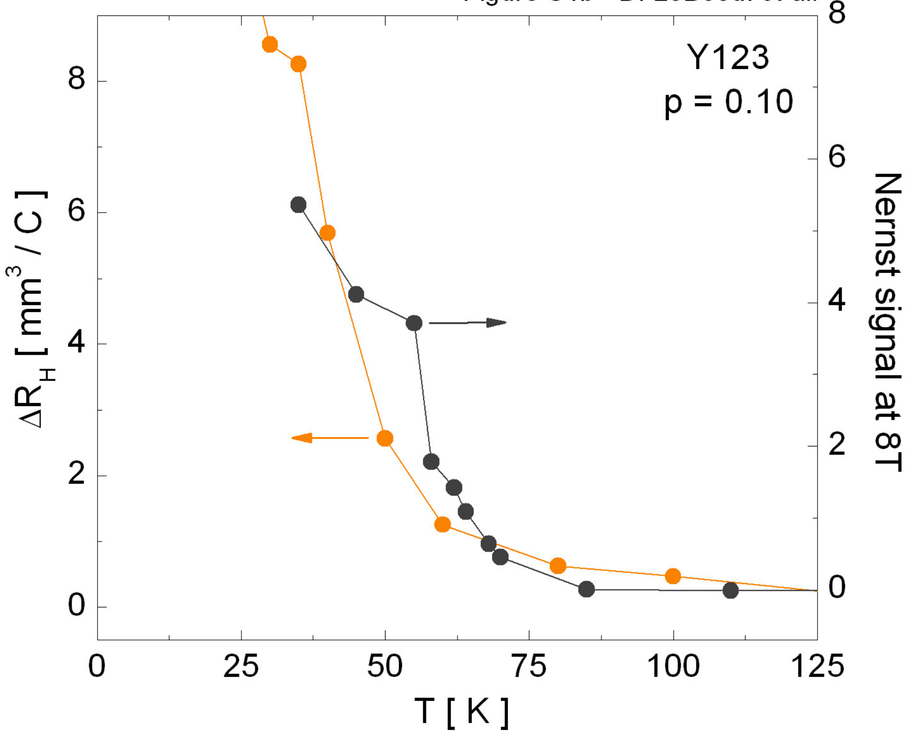

Figure S5 | Hall resistance in $NbSe_2$.

Hall resistance R_{xy} normalised at 60 K as a function of temperature for a pure and a dirty sample of $NbSe_2$ (from ref. 7: samples Q and D, respectively). The vertical dashed line marks the transition to the charge-density-wave phase in $NbSe_2$ at $T_{CDW} \approx 30$ K.